

# A review of maximum power point tracking techniques for use in partially shaded conditions



Yi-Hua Liu<sup>a,\*</sup>, Jing-Hsiao Chen<sup>a</sup>, Jia-Wei Huang<sup>b</sup>

<sup>a</sup> Department of Electrical Engineering, NTUST, Taipei, Taiwan, ROC

<sup>b</sup> Photovoltaic Technology Division System Application Dept. Green Energy & Environment Research Lab., ITRI, Hsinchu, Taiwan, ROC

## ARTICLE INFO

### Article history:

Received 10 November 2013

Received in revised form

7 August 2014

Accepted 17 August 2014

### Keywords:

Maximum power point tracking (MPPT)

Photovoltaic generation systems (PGS)

Partially shaded conditions (PSC)

## ABSTRACT

Partially shaded conditions (PSCs) often occur in large photovoltaic generation systems (PGSs). PSCs cause losses in system output power, hot spot effects, and system safety and reliability problems. When PSC occur, the PGS power–voltage characteristic curve exhibits multiple peak values; that is, the curve comprises a global maximum power point and multiple local maximum power points. Current literature includes various studies of global maximum power point tracking (GMPPT) algorithms and hardware architectures suitable for PSC; because the substantial quantity of PSC literature, this subject must be comprehensively reviewed. To focus on GMPPT techniques used in PSC, traditional maximum power point tracking techniques and circuit architectures that cannot distinguish GMPP and LMPP were not discussed.

© 2014 Elsevier Ltd. All rights reserved.

## Contents

1. Introduction	437
2. Exploration of the effects of partially shaded conditions	437
2.1. Basic characteristics of PV cells	437
2.2. Effect of partial shade conditions on photovoltaic generation systems	437
3. Global maximum power point tracking techniques for partial shading conditions	437
3.1. Firmware-based GMPPT techniques	437
3.1.1. Two-stage method	437
3.1.2. Segmental search method	440
3.1.3. Soft computing method	441
3.1.4. Other methods	444
3.1.5. Comparing firmware-based methods	445
3.1.6. Methods for detecting partial shading condition	445
3.2. Hardware-based GMPPT techniques	445
3.2.1. Investigation on system configuration and reconfiguration technique	445
3.2.2. Multi-level converter	445
3.2.3. Distributed architecture	447
3.2.4. Equalizer-assisted architecture	447
3.2.5. Summary and comparison of hardware methods	447
4. Simulated results of selected methods	447
5. Conclusion	450
Acknowledgments	450
References	450

\* Corresponding author.

## 1. Introduction

According to a technical report by the European Photovoltaic Industry Association (EPIA), more than 31 GW of photovoltaic (PV) capacity was installed globally in 2012; aggressive projections indicate that this number could increase to 84 GW in 2017 [1]. Weather and environmental factors affect the output characteristics of PV cells, that is, cell output voltage and current vary according to changes in irradiance and temperature. Therefore, a unique maximum power point (MPP) exhibits under specific irradiance and temperature. The maximum power point tracking (MPPT) algorithm is crucial in attaining the maximal PV power, facilitating optimal PV cell performance. Researchers have proposed numerous MPPT algorithms that demonstrate excellent tracking efficiency in uniform insolation conditions. However, PV generation systems (PGSs) in urban environments installed on rooftops or eaves are easily shaded by neighboring buildings, clouds, or dust coverage, causing PGSs to generate power output that differs from that in ideal insolation conditions. Shading is especially problematic regarding PGSs that exhibit wide-range layouts primarily because complete shading of a large area is unlikely, causing partially shaded conditions (PSC). When PSC occur, certain PV cells are exposed to normal, non-shaded conditions, and output normal power levels; however, other cells yield decreased output levels because of shading, generating a mismatch in the overall PGS. Because of the characteristics of PV cells, shaded conditions significantly reduce cell output current but not output voltage. This mismatch in power generation influences series-connected PGSs; however, traditional MPPT algorithms are designed to address only uniform insolation and cannot adequately account for PSC. Consequently, developing new MPPT techniques suitable for application in PSC is critical. Numerous studies regarding this subject have been published; thus, composing an accurate and comprehensive reference document that details information related to various MPPT techniques applicable to PSC is essential.

Various reviews [2–10] of MPPT methods for PGSs exist in the current literature; of these studies, most of the reviews [2–7] researched only traditional MPPT methods, and Ishaque and Salam [8] and Salam et al. [9] focused on both traditional methods and those suitable for PSC. When PSC occur, the power–voltage ( $P$ – $V$ ) characteristic curve of the PV modules becomes complex, exhibiting multiple peak values. Therefore, traditional MPPT methods are not suitable for use in PSC. To provide PGS researchers and engineers with useful reference information, this study explored global maximum power point tracking (GMPPT) methods suitable for application in PSC. First, the basic operating principles of various GMPPT methods, including their advantages and limitations, were described. Regarding firmware-related techniques, various indices were evaluated, including whether the design parameters were relevant to the system, GMPPT time, GMPPT accuracy, algorithm complexity and required sensors. In terms of hardware-related techniques, the advantages and disadvantages of various architectures were discussed. Finally, an in-depth simulation on some highly cited GMPPT methods was made and conclusion was offered accordingly. It was difficult to propose a fair benchmark for various techniques mentioned in the literature primarily because researchers used distinct PGSs (including power rating and power converter topology) and shading patterns to test their proposed algorithms. Nonetheless, the authors of the current study endeavored to employ several fair evaluation indices and verify the correctness of this performance evaluation using the simulated results in Section 4. The information gathered herein should provide researchers with comprehensive reference information and recommendations for future studies addressing PSC. Although Bidram et al. [10] also compared GMPPT methods, this

study additionally classified various GMPPT methods into categories and explored their usage limitations and design considerations. Furthermore, shading detection methods proposed in the literature were compared, and a simulation platform was provided for verifying the performance of some highly cited GMPPT methods. To the best of the authors' knowledge, no existing literature has provided this type of categorizing and testing.

## 2. Exploration of the effects of partially shaded conditions

When PV cells are connected in series, a bypass diode is typically added in parallel for protection, preventing damage due to overheating when one or more PV cells are shaded or shorted. However, adding a bypass diode changes the current–voltage ( $I$ – $V$ ) characteristic curve when the PGS is shaded by environmental conditions such as clouds, tree shade, and building shadows. Furthermore, the  $P$ – $V$  characteristic curve also changes accordingly and exhibits multiple peak values. Current studies on the effects of PSC can be divided into three categories: (1) deriving analytical mathematical formulas to describe the  $I$ – $V$  and  $P$ – $V$  characteristic curve [11,12]; (2) establishing a simulation or experimental platform that can evaluate the effects of PSC [13–20]; and (3) evaluating the power losses caused by PSC [21–25]. This section explores the effects of PSC in PGSs.

### 2.1. Basic characteristics of PV cells

Based on their electrical characteristics, PV cells are equivalent to a one-diode model as shown in Fig. 1. This model includes a current source  $I_s$ , a diode current  $I_d$ , an equivalent parallel resistance  $R_p$ , and an equivalent series resistance  $R_s$ . The output current of the PV module  $I_{PV}$  is the difference between the photogenerated current  $I_s$  and diode current  $I_d$ , as shown in (1):

$$I_{PV} = I_s - I_{S0} \left( \exp \left( \frac{q(V_{PV} + I_{PV}R_s)}{akT} \right) - 1 \right) - \frac{V_{PV} + R_s I_{PV}}{R_p} \quad (1)$$

where  $I_{S0}$  is the saturation current,  $V_{PV}$  is the output voltage of PV module,  $q$  is the charge of a single electron,  $a$  is the ideal factor of the diode,  $k$  is the Boltzmann constant,  $T$  is the temperature in Kelvin.

### 2.2. Effect of partial shade conditions on photovoltaic generation systems

PGSs are formed by several PV modules, which comprise several PV cells connected in series or parallel. Parallel connections can increase the output current of the module, and serial connections can improve the output voltage. When PSC occur, the shaded PV cell becomes a load instead of a generator, producing a hot spot that can subsequently destroy PV cells. Therefore, commercially available PV modules often comprise a parallel-connected bypass diode to prevent this problem. When PSC occur, currents flow through the bypass diode instead of the shaded PV module, generating multiple steps in the  $I$ – $V$  characteristic curve and

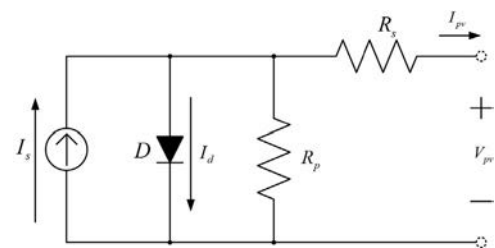


Fig. 1. Equivalent circuit of photovoltaic cells.

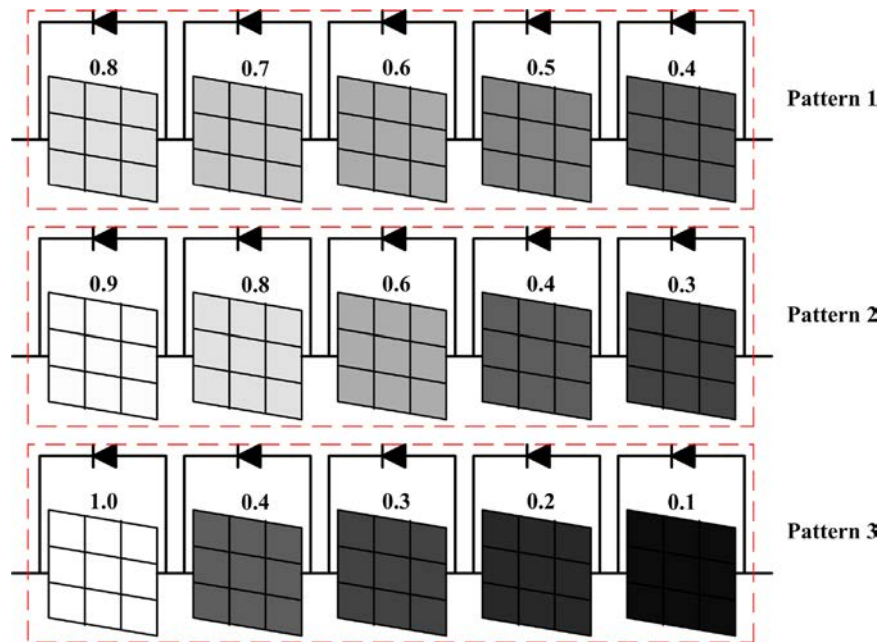


Fig. 2. A 5s1p PGS with various shading patterns.

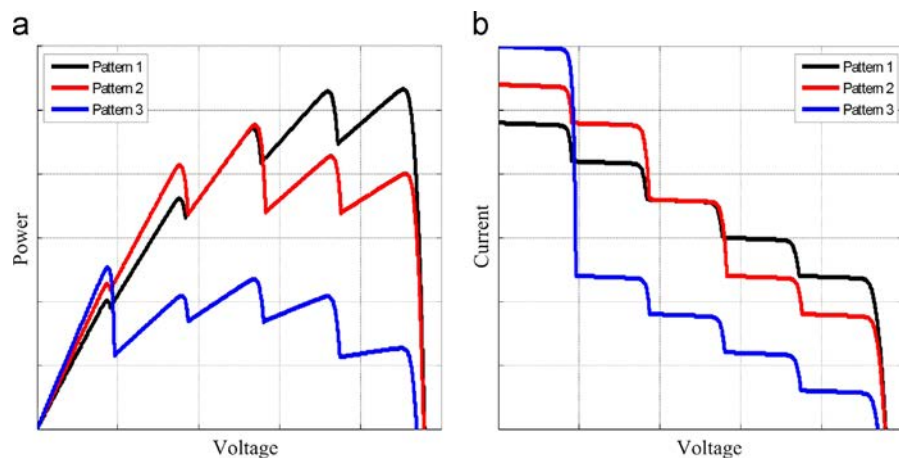


Fig. 3. The characteristic curves of the 5s1p PGS in Fig. 2: (a)  $P$ - $V$  characteristic curve; (b)  $I$ - $V$  characteristic curve.

multiple peak values in the  $P$ - $V$  characteristic curve. For example, Fig. 2 shows a PGS comprising five PV modules connected in series (denoted as 5s1p system). Its  $P$ - $V$  and  $I$ - $V$  characteristic curves for different shading patterns are illustrated in Fig. 3(a) and (b), respectively. Fig. 3 shows that GMPP under PSC may occur on a larger voltage range compared with that in PGSs under uniform insolation.

### 3. Global maximum power point tracking techniques for partial shading conditions

In this section, GMPPT techniques suitable for PSC are explored. The solutions for PSC proposed in current literature can be divided into firmware-based [26–69], and hardware architecture-based solutions [70–113]. Fig. 4 displays common PGS architectures, illustrating that when PGSs use a centralized architecture, only one set of power converter is required; therefore, firmware must be used to address the multiple peak values that the PSC cause in  $P$ - $V$  characteristic curves. On the other hand, when PGSs use distributed architectures, multiple sets of power converter exist; therefore, each power converter can track its own MPPT. Because

hardware-based solutions relate to the power converter topology and system design, this study mainly focuses on exploring firmware-based GMPPT techniques. Fig. 5 shows the  $P$ - $V$  characteristic curve of a typical 5s1p system under a specific shading pattern; this system was used as the basis to clarify operating concepts and design guidelines regarding various GMPPT algorithms. (Fig. 6).

#### 3.1. Firmware-based GMPPT techniques

##### 3.1.1. Two-stage method

Fig. 5 shows that when PSC occur, the  $P$ - $V$  characteristic curve of PGS exhibits multiple peak values, and the number of peak values correlates with the shading pattern. By dividing this  $P$ - $V$  characteristic curve into multiple single-peak  $P$ - $V$  characteristic curves, traditional MPPT methods (e.g., perturb & observe (P&O) or incremental conductance (IncCon) methods) can be used to determine the maximal value of each single-peak curve. Therefore, the two-stage technique involves using methods proposed in the first stage to determine the approximate GMPP location (i.e., an interval), subsequently using traditional MPPT methods to determine the precise GMPP location. Thus, the key to the success of the

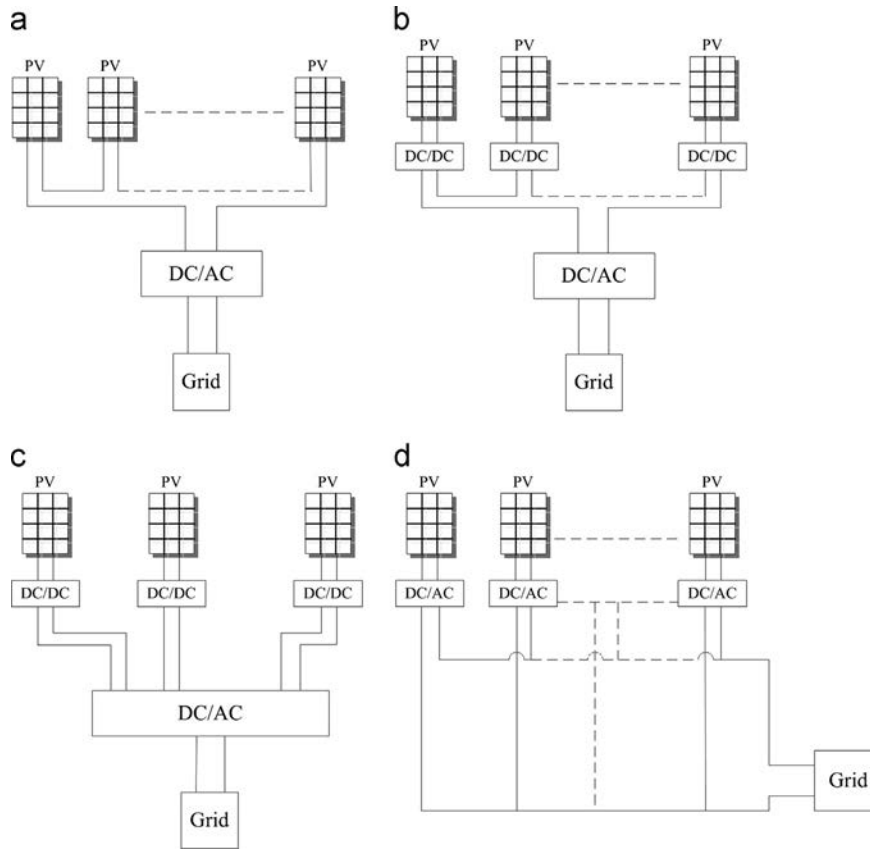


Fig. 4. Common PGS architectures.

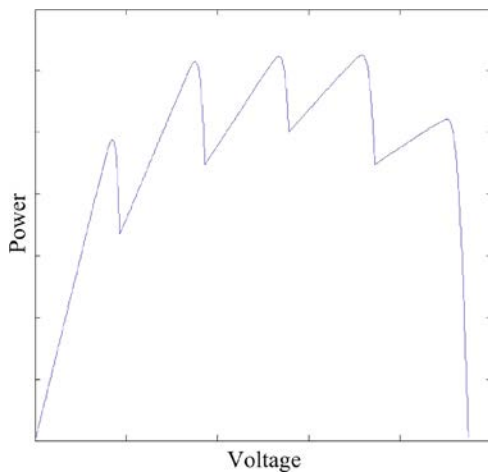


Fig. 5. P–V characteristic curve under a specific shading pattern.

two-stage method is the accuracy of the GMPP interval obtained in the first stage. The following sections clarify the two-stage method used in the literature.

3.1.1.1. *System characteristic curve method.* Works in [26–28] employed a similar technique, using a preset linear function to move the operating point (OP) near the GMPP under PSC, as shown in Fig. 7. This linear function is related to various system parameters, including open circuit voltage and short circuit current. The linear function used in [26] can be expressed as follows:

$$R_{pm} = \frac{V_{pm}}{I_{pm}} \quad (2)$$

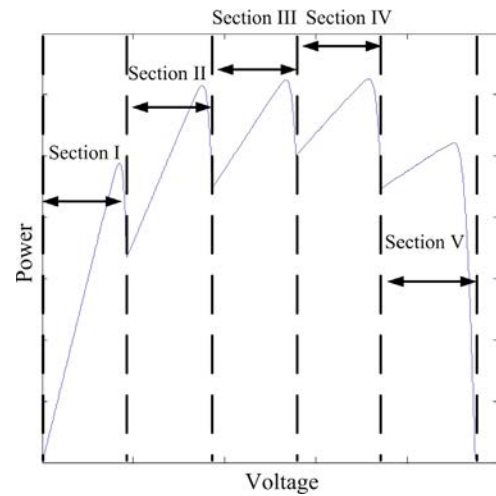


Fig. 6. Concept of dividing multiple-peak P–V characteristic curve into several single-peak curve.

The linear function used in [27] can be expressed as follows:

$$P_{MPP}(t) = a[T(t)]I_{MPP}[E(t)] \quad (3)$$

And the linear function used in [28] can be expressed as follows:

$$V_{pv}^* = \left(\frac{V_{o,rms}}{I_{o,rms}}\right) \times I_{pv}[n] \approx \left(\frac{V_g}{I_{out}}\right) \times I_{pv}[n] \quad (4)$$

The advantage of this method is its tracking speed. Because the first stage only requires one step to move the OP to the vicinity of the GMPP, the tracking time of this method is similar to that of traditional MPPT methods. However, disadvantages exist. First,



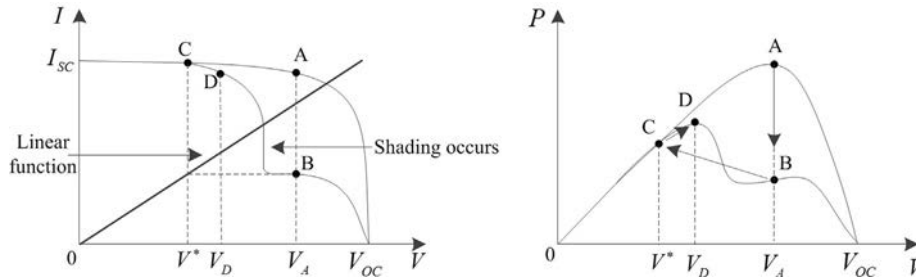


Fig. 7. System characteristic curve method.

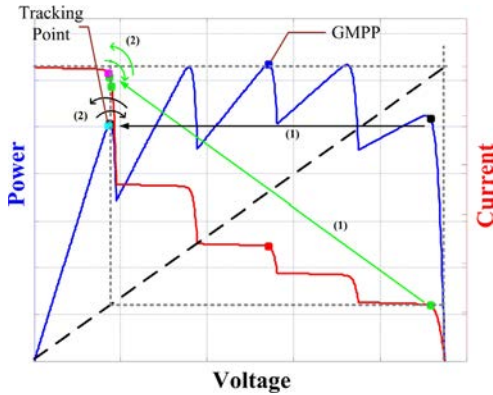


Fig. 8. Incorrect tracking of GMPP using the system characteristic curve method.

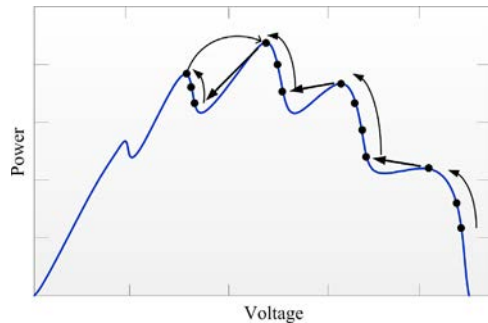


Fig. 9. Method proposed by Patel.

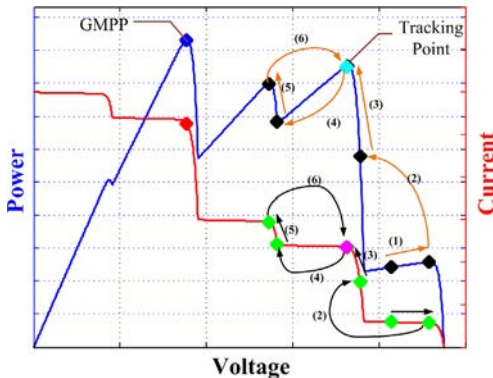


Fig. 10. Incorrect tracking of GMPP using the method proposed by Patel.

obtaining the open circuit voltage and short circuit current of the system requires open or short circuits. Implementing this in an actual system can cause power losses or safety concerns. Second, although the linear function used in this method can move the OP near the GMPP in certain shading patterns, an erroneous location of the new OP can prevent tracking the GMPP; thus, this method cannot guarantee that the GMPP can be tracked. This concept is

shown in Fig. 8. Furthermore, when shading patterns become complex, the probability that this method can successfully track GMPP decreases. Ref. [29] is one conference paper that used a concept similar to this method.

3.1.1.2. Two-stage searching method. In a two-stage searching method, the first stage is used to search for the GMPP location interval; traditional MPPT methods are then used in the second stage to find the precise GMPP location. By using this method, Patel and Agarwal [30] employed various shading pattern observations as clues to determine the GMPP location. As shown in Fig. 9, the basic search rules for [30] are as follows:

- 1)  $0.85 V_{oc,all}$  ( $V_{oc,all}$  represents the total open circuit voltage of the system) is used as the P&O search starting point to find and record a peak value.
- 2) The peak value found in Step 1 is used as the basis for moving the OP one large step (the reference recommended  $0.6-0.7 V_{oc,one}$  ( $V_{oc,one}$  represents the open circuit voltage of a single module)) to the left, then conduct P&O to search and record the next peak value.
- 3) If the obtained peak value is higher than the previous peak value, Step 2 is repeated; if the determined peak value is smaller than the previous peak value, then the previous peak value is the GMPP.

Ref. [30] is the paper with the highest number of citations among similar literature; its method is easy to implement, and can be integrated into traditional PGS firmware; however, disadvantages exist. First, the authors of [30] found that when  $P-V$  curve is traversed from either side, the magnitude of the peaks increases; after reaching the GMPP, the magnitude of the subsequent peaks continuously decreases. Therefore, Step 3 can be used to determine the GMPP. However, the current study explored all possible shading patterns and found that there exists some exception about this claim (for detailed descriptions, please refer to Section 4). Consequently, this method cannot ensure successful GMPPT. Fig. 10 shows one example of this exception. In addition, the parameter used in this method (i.e. value of the large step) affects the probability of tracking the GMPP. Another disadvantage of this method is the tracking speed. Because each LMPP must be determined using P&O method, this method requires more tracking steps compared with other methods.

Works in [31–33] used similar methods, employing a large interval to search the entire  $P-V$  characteristic curve (called global-biased search) to determine the largest peak value. Next, a refined search is conducted around the largest peak value found in previous stage to locate the GMPP (called local-biased search). Of these three approaches, Renaudineau et al. [31] used  $\alpha$ , Koutroulis et al. [32] used fixed power intervals, and Kouchaki et al. [33] used  $0.8 V_{oc,one}$  as the step for global-biased search. The concept of this kind of method (Ref. [32] by Koutroulis) is shown in

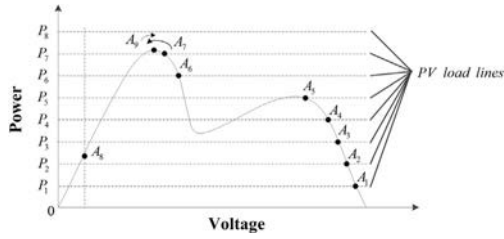


Fig. 11. Method proposed by Koutroulis.

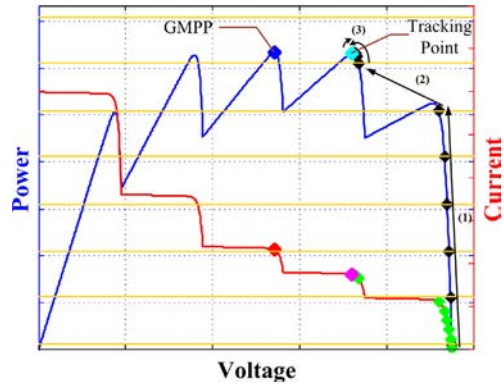


Fig. 12. Incorrect tracking of GMPP using the method proposed by Koutroulis.

Fig. 11. The advantage of this kind of method is its simplicity; it can easily be integrated with traditional PGS firmware (requiring only an additional global-biased search stage). The disadvantage of this kind of method is that the selected global-biased search step affects the probability of finding the GMPP. When the selected step is large, the system requires comparatively less time to locate the GMPP, but may miss the GMPP, as shown in Fig. 12. Conversely, when a small step is selected, the system has an increased probability of finding the GMPP, but requires relatively more time. To use this method, a tradeoff between the search step size and the time required must be addressed (for details, please refer to Section 4). In addition, the method in [32] used power as the step variable for the search. Although this thinking is intuitive and yields a comparatively fast tracking speed, this method requires using a specifically designed power converter that can accept power command for constant power control. Kashif et al. [34] and Kouchaki et al. [35] are conference papers used similar two-stage searching concepts.

3.1.2. Segmental search method

The basic principle of the segmental search method is similar to that of the two-stage searching method described in 3.1.1.2. The primary difference is that two-stage searching method uses traditional MPPT methods (such as P&O) as the basis for the second stage search. Segmental search, however, is based on mathematical theories, finding the GMPP by gradually reducing the search range.

3.1.2.1. DIRECT method. The theoretical basis for the method used in [36] is that the P–V characteristic curve of PV modules conforms to Lipschitz characteristics; therefore, the dividing rectangle (DIRECT) technique can be used to find the peak values. DIRECT refers to dividing the search area into three areas of equal intervals by using mathematical methods, subsequently using mathematical equations to find potentially optimal intervals (POIs) that exhibit

potential peak values. The rules for POI search are as follows:

$$f(x_j) + \tilde{K} \frac{(a_j - b_j)}{2} \geq f(x_i) + \tilde{K} \frac{(a_i - b_i)}{2} \quad \forall i \tag{5}$$

$$f(c_j) + \tilde{K} \frac{(a_j - b_j)}{2} \geq f_{\max} + \varepsilon |f_{\max}| \tag{6}$$

The search area is divided into three equal portions to locate the POIs before further subdivision, as shown in Fig. 13.

Ref. [36] has been frequently cited and compared. The advantage of this method is that it is based on a solid mathematical foundation and facilitates rapid tracking; its disadvantages are similar to those of the two-stage searching method. In certain shading patterns, this method cannot track the GMPP, although this is unlikely. Another potential disadvantage is that although the mathematical equations used in this method are relatively simple and the segmentation concept can be easily implemented, the author added numerous exceptions during actual implementation to avoid missing the GMPP. For example, the author proposed conducting nine interval searches within the search range; however, if the POIs that contained the two largest values were not adjacent to each other, then a wide area search with 27 intervals had to be re-conducted. Conversely, if the obtained POIs were adjacent to each other, then segmentation could be conducted on the POI with the maximal value. This type of exception adds complexity and difficulty when firmware engineers implement the algorithm based on the DIRECT method. In addition, this method cannot be directly integrated into traditional PGS firmware.

3.1.2.2. Fibonacci methods. Works in [37] and [38] used Fibonacci sequences as a basis for GMPP searches. Compared with the DIRECT method in 3.1.2.1, the primary difference of this method is using the Fibonacci sequence as the mathematical basis for segmentation, as shown in Fig. 14. The equation is as follows:

$$x_2 = x_3 + \left[ \frac{F(n-1)}{F(n)} \right] (x_4 - x_3) \tag{7}$$

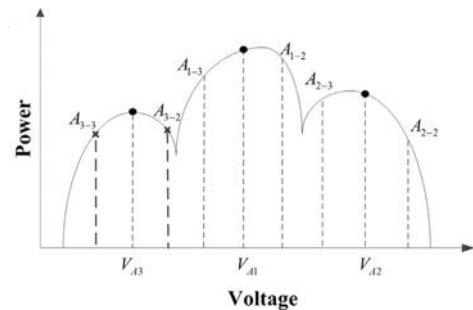


Fig. 13. The concept of DIRECT method.

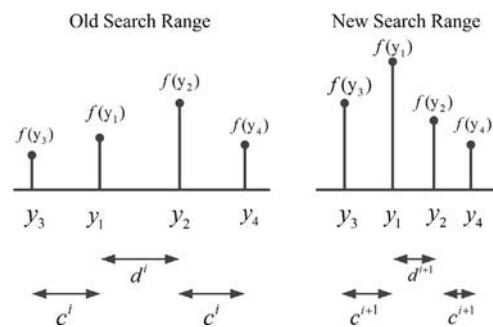


Fig. 14. The concept of the Fibonacci method.

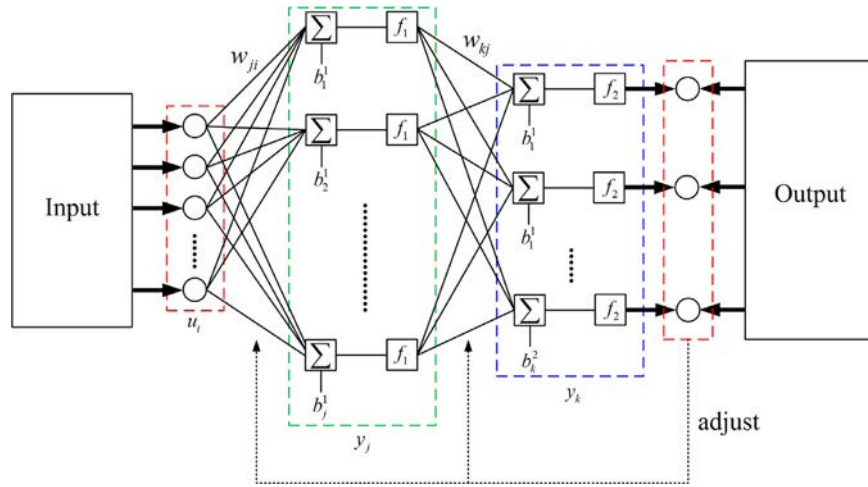


Fig. 15. ANN with three layers (one hidden layer).

$$x_1 = x_4 + \left[ \frac{F(n-1)}{F(n)} \right] (x_4 - x_3) \quad (8)$$

where  $F(n-1)$  and  $F(n)$  represent the  $(n-1)$ th and  $n$ th number in the Fibonacci sequence. The advantages and disadvantages of this method are the same as those in the DIRECT method.

Ref. [39] and Ref. [40] are conference papers related to the segmental search method. Fan et al. [39] used a random number method to randomly sample power values under six distinct voltages, subsequently using the point with the highest power value (of the six selected points) to determine the new search range. Repeat random sampling was conducted on the new range until convergence was achieved. Escobar et al. [40] used the geometric characteristics of the  $I-V$  characteristic curve to conduct a sweep search with variable steps.

### 3.1.3. Soft computing method

Soft computing (SC) refers to using computers to simulate the biochemical processes of natural intelligence systems (e.g., human perception, brain structure, and evolutionary process) to solve non-deterministic polynomial-time hard (NP-hard) or NP-complete problems. Because finding the GMPP in multi-peak  $P-V$  characteristic curves caused by PSC can be viewed as an optimization problem, scholars have used SC techniques to address such problems. SC methods include artificial neural networks (ANNs), fuzzy logic control (FLC), evolutionary computation (including genetic algorithms (GAs), differential evolution (DE), particle swarm optimization (PSO), ant colony systems (ACSS)), and chaotic search (CS).

**3.1.3.1. Artificial neural network.** An ANN is a computational model that uses interconnected artificial neurons to imitate the ability of biological neural networks. An ANN with three layers is shown in Fig. 15. From Fig. 15, users can input information (such as irradiance level and the temperature of PV modules) into the input layer and calculate the output (such as the GMPP location) according to the weighting values of ANN. For example, the input and output relation of an ANN as shown in Fig. 15 can be obtained using (9) to (12). The neurons in the input layer are responsible only for transmitting the input information to the hidden layer. The input of the number  $j$  unit in the hidden layer can be

expressed as follows:

$$n_j^1 = \sum_{i=1}^5 w_{ji} u_i + b_j^1 \quad (9)$$

where  $w_{ji}$  is the weighting of the  $i$ th input unit connected to the  $j$ th hidden layer unit, and  $b_j^1$  represents the bias value of the  $j$ th unit in the hidden layer. The output of the  $j$ th unit in the hidden layer can be expressed as follows:

$$v_j = f_1(n_j^1) \quad (10)$$

where  $f_1$  is the activation function used in this layer. Commonly used activation functions include linear function, hyperbolic tangent sigmoid, and Log-sigmoid. Notably, if a low-cost microcontroller with low calculation capability is used to implement the ANN, the linear function is preferred because it is relatively easy to apply.

The input of the  $k$ th unit in the output layer can be expressed as follows:

$$n_k^2 = \sum_{j=1}^{10} w_{kj} v_j + b_k^2 \quad (11)$$

where  $w_{kj}$  is the weighting value of the  $j$ th hidden layer unit connected to the  $k$ th output unit, and  $b_k^2$  represents the bias value of the  $k$ th output unit. The output of the  $k$ th output unit can be expressed as follows:

$$v_k = f_2(n_k^2) \quad (12)$$

Similarly,  $f_2$  is the activation function used for the output layer.

By using large amounts of training data, the ANN continually adjusts the weighting and bias values, allowing the network-calculated output to approximate the target output. One of the most common ANN learning methods is the back-propagation method. The advantage of ANNs is their parallel computing capability. Other SC methods may require multiple iterations to obtain the optimal solution, whereas ANNs can use simple multiplication and addition to rapidly calculate output. Therefore, ANNs enable rapid calculation. However, the accuracy of an ANN is determined based on its training data. If the training data are insufficient, or the data do not cover the entire problem space, then the accuracy of the ANN will be reduced accordingly. Currently, the ANN-based MPPT method can only be used in uniform insolation conditions [41,42] primarily because at a single



irradiance level, the location of the MPP is only related to the irradiance and the temperature. Thus, the training data are simple. When PSC occur, the irradiance of the module, module temperature and shading pattern all affect the MPP location. Consequently, the training data required by the ANN substantially increase, and these data are not easily collected. This is the primary limitation of applying ANNs to GMPP searches. Therefore, only works in [43] and [44] in current literature proposed using ANNs as the primary method for addressing PSC. The input variables used in [43] and [44] were the averaged irradiance of selected modules, and the design was affected by the arrangement method of PV modules. Therefore, if the architecture of the PV array changes (e.g., adding new PV panels), the ANN must be re-trained. In addition, irradiance and temperature sensors are more expensive compared with the voltage and current sensors used in other GMPP methods. Ref. [45] is one conference paper that used ANN concepts.

**3.1.3.2. Fuzzy logic control.** Traditional control system design requires understanding the system being controlled; that is, using precise mathematical models to describe the system. However, when the controlled system becomes overly complex, it is often difficult to use system identification method to establish a system model. On the other hand, FLC uses fuzzy set theory to convert the linguistic values directly into automatic control strategies using expert knowledge or operator experience. The advantages of FLC include the following: 1) no precise mathematical model is required; and 2) FLC can integrate the knowledge of human experts into the controller design process. When conducting fuzzy control, the behavior of the system being controlled is described by a set of fuzzy rules. These fuzzy rules use semantic fuzzy information rather than mathematical equations. Therefore, FLC can convert the knowledge of human experts into fuzzy control rules, reducing the complexity of control system design. Fig. 16 shows a typical block diagram of FLC. From Fig. 16, a FLC comprises three primary parts: fuzzification stage, a fuzzy inference engine, and defuzzification stage. In the fuzzification stage, membership function is used to convert the input data into linguistic values. The fuzzy inference engine must be used in conjunction with the fuzzy rule base, and can be used to calculate the required control quantity. In the defuzzification stage, mathematical equations are used to convert the output variable from a linguistic value to a crisp value. The center of gravity and center of area methods are often used for defuzzification. Regarding FLC, establishing a rule base is critical in the design. The if-then rules formed using linguistic variables can be employed to establish the FLC system input and output relations, and must be designed to agree with the knowledge of experts concerning a specific problem. FLC is particularly suitable for use in non-linear, time-varying systems and systems with incomplete models. Thus, FLC can be used to deal with PSC problems. Karatepe et al. [46] used distributed architecture and utilized FLC to replace traditional MPPT methods.

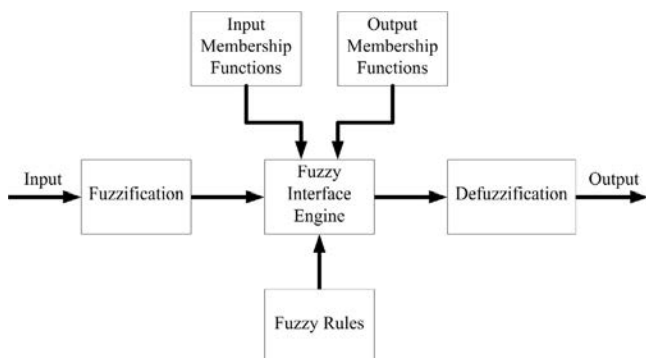


Fig. 16. Basic FLC framework.

Because each power converter contains a designated MPPT controller, the system guarantees that the GMPP can be tracked. The advantage of the method used in [46] is its rapid tracking speed and high tracking accuracy; its disadvantage is that it exhibits a higher hardware cost compared with that of centralized architectures. Alajmi et al. [47] used a method similar to the two-stage searching method in 3.1.1.2 to conduct GMPPT. This method first swept the P–V characteristic curve and recorded various LMPPs, then replaced P&O by using FLC to conduct GMPPT. This method yields a rapid tracking speed, but demonstrates disadvantages similar to those of other two-stage searching methods. Ref. [48] is one conference paper that used FLC concepts.

**3.1.3.3. Genetic algorithm.** A GA is an evolutionary computation (EC) method that mimics the “survival of the fittest” evolutionary law in the natural world; its primary operators are reproduction, crossover, and mutation. The process of using GA to obtain the optimal solution for a problem is as follows: 1) the search parameters are coded as binary strings in a chromosome; 2) this process is randomly repeated to produce N initial species (strings); 3) the fitness function is designed based on the solution conditions. Species that exhibit high fitness values are selected for the mating pool (i.e., the reproduction process); and 4) the crossover and mutation processes are computed to complete one generation of GA. This process is repeated to produce the species with the highest fitness value, as shown in the evolutionary process in Fig. 17. GA has been used to optimize the parameters of other algorithms (such as FLC or ANNs); only Shaiek et al. [49] used GA to solve PSC problems. Compared with other EC methods, implementing GA is complex and difficult to achieve using low-cost microcontrollers. Consequently, Ref. [49] only provided simulated results. Ref. [50] is one conference paper that used GA concepts.

**3.1.3.4. Differential evolution.** DE is also an EC method, and uses architecture similar to that of GA. The primary difference is that DE uses special differential operators to replace the crossover process in GA and produce the next generation. Comparing to GA, DE is simple to implement and requiring few parameter adjustments. Currently, no journal paper has used DE to solve PSC problems.

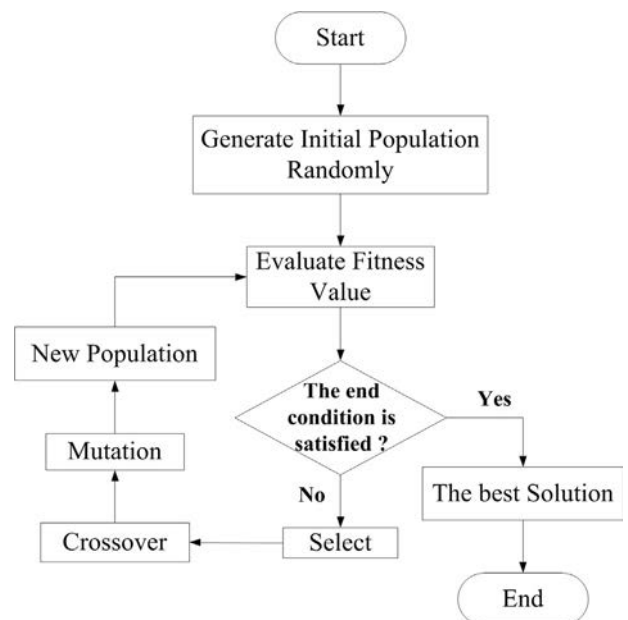


Fig. 17. The evolutionary process of GA.



Ref. [51] and Ref. [52] are conference papers based on DE, and they provided only simulated results.

**3.1.3.5. Ant colony system.** An ACS is an EC method based on swarm intelligence; its primary advantage is immediately adapting command values according to environmental changes. Thus, ACSs are suitable for conducting MPP tracking in changing environments. In an ACS, each agent selects its path randomly at first. If the path the agent chooses is short (has high fitness value), the agent leaves concentrated pheromone on the path. In the next iteration, the agent chooses its path based on the concentration of pheromone on that path. The more concentrated the pheromone is, the higher probability is that the agent chooses that path. The probability of the agent moving from position  $i$  to position  $j$  is as follows:

$$P_{ij}^k = \frac{\tau_{ij}^\alpha \eta_{ij}^\beta(t)}{\sum_{s \in \text{allowed}_k} \tau_{ij}^\alpha \eta_{ij}^\beta(t)} \quad (13)$$

where  $\tau_{ij}$  is the pheromone quantity on path  $(ij)$ ,  $\eta_{ij}$  is the initial value of pheromone on path  $(ij)$ ,  $\alpha$  and  $\beta$  are adjustable parameters, and the updated pheromone equation can be expressed as follows:

$$\tau_{ij}(t+n) = \rho\tau_{ij}(t) + \Delta\tau_{ij} \quad , \quad \Delta\tau_{ij} = \sum_{k=1}^m \Delta\tau_{ij}^k \quad (14)$$

In (14),  $\Delta\tau_{ij}^k$  represents the quantity of pheromone that the  $k^{\text{th}}$  agent left on path  $(ij)$  in this iteration, whereas  $\tau_{ij}^k$  represents the total pheromone quantity left on path  $(ij)$ .  $\rho$  is a coefficient such that  $(1-\rho)$  represents the evaporation rate. The frequently used  $\Delta\tau_{ij}^k$  calculation method is as follows:

$$\Delta\tau_{ij}^k = \begin{cases} \frac{Q}{L_k} & , \text{ if the } k\text{-th ant passes path } (i,j) \text{ in this iteration} \\ 0 & , \text{ other} \end{cases} \quad (15)$$

In (15),  $Q$  is a constant and  $L_k$  represents the distance of the path that the  $k^{\text{th}}$  agent passes in this iteration.

Based on the principle represented by the mentioned equations, Jianga et al. [53] used ACS to solve GMPPT problems. However, ACSs are difficult to implement using low-cost micro-controllers; therefore, Ref. [53] provided only simulated results.

**3.1.3.6. Particle swarm optimization.** PSO is also an EC method based on swarm intelligence. In the PSO method, each particle is defined by its own position and velocity. The behavior of particles within the swarm is influenced by the experiences of neighboring particles. Each particle follows the current best-performing particle to search within the solution space. In the PSO method, particles are initially randomly or evenly distributed in the solution space. In each iteration, particles follow two “extreme values” to update themselves. The first value is the optimal solution that the particle found, also called the personal best value (pbest); the second extreme value is the optimal solution discovered by the entire swarm, also called the global best value (gbest). After these optimal solutions are found, the particles update their velocity and position based on the following equations, as shown in Fig. 18:

$$v_i^{k+1} = wv_i^k + c_1 \text{rand}_1^k (\text{pbest}_i^k - x_i^k) + c_2 \text{rand}_2^k (\text{gbest}^k - x_i^k) \quad (16)$$

$$x_i^{k+1} = x_i^k + v_i^{k+1} \quad (17)$$

Where  $v_i^k$  is the velocity of particle  $i$  of the  $k^{\text{th}}$  iteration;  $w$  is the weight value;  $c_1$  and  $c_2$  are acceleration coefficients (also called

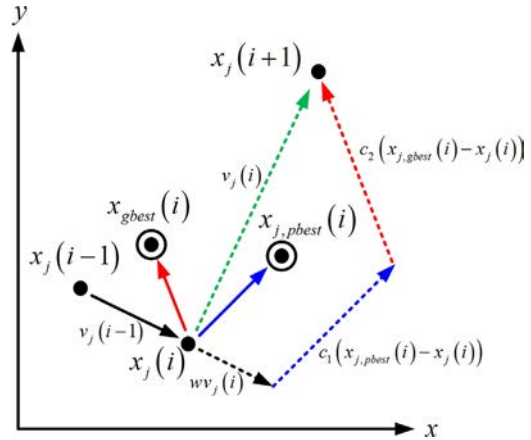


Fig. 18. Concept of updating the searching path for PSO.

learning factors), which were used to direct the search toward the local and global optimal solutions, respectively; and  $\text{rand}_1$  and  $\text{rand}_2$  are random numbers between  $[0, 1]$ .

Of all the EC methods, the PSO algorithm is most widely applied to GMPPT. Because PSO is an optimization method based on swarming, it can conduct GMPPT in distributed architecture [54–56] or centralized architecture [57–60]. Regarding algorithms, Chowdhury and Saha [54] used adaptive perceptive PSO (APPSO), whereas the remaining references used basic PSO algorithms. Because implementing APPSO is complex, Ref. [54] provided only simulated results, whereas the remaining references provided experimental results. This observation shows that the PSO algorithm is an EC method that can be readily implemented using microcontrollers. In terms of centralized architecture, the PSO method can accurately track the GMPP in various shading patterns, conduct direct cycle control [57–60], and attain reduced steady-state oscillation [58]. In [60], random number in the accelerations coefficient is removed, developing a deterministic PSO (DPSO) mechanism that improved the tracking speed. In addition, Liu et al. [59] proposed suggestions regarding practically implementing PSO.

Conference papers [61–64] involved similar PSO methods; authors in [63] and [64] combined PSO and Bayesian fusion, rendering a system that can yield excellent GMPPT results in a changing environment.

**3.1.3.7. Chaos search method.** CS is a stochastic search method based on chaos theory, using the ergodicity of the chaos variable to conduct an optimization search. Consequently, the search results of this method are superior to those of other search methods using pure random numbers. Zhou et al. [65] used CS method based on dual carrier to conduct GMPPT search, employing (18) and (19) to randomly produce control variables, measure output power, and find the GMPPT:

$$x_i^r = a + x_n(b - a) \quad (18)$$

$$y_i^r = a + \frac{1}{\Lambda}(y_n + 2)(b - a) \quad (19)$$

According to [65], CS can accurately find the GMPPT under PSC; however, simulated and experimental results did not verify this theory.

**3.1.3.8. Tabu search method.** The Tabu search method used records of previous search results to avoid falling into local optimal solutions. Zheng et al. [66] proposed using tabu search to solve GMPPT search problems; however, the authors did not conduct an in-depth exploration of its implementation or design guidelines.

3.1.4. Other methods

This subsection introduces additional GMPPT techniques that were not categorized into the three previous subsections.

3.1.4.1. *Extreme seeking control method.* The extreme seeking control (ESC) method is an adaptive close-loop control method used to search for extreme values. Compared with traditional P&O, ESC enhances tracking speed. Fig. 19 shows the block diagram of a typical ESC. To address PSC, Lei et al. [67] used a method similar to that of [30] to sweep and search for the GMPP location. The largest difference between this method and that of [30] is that it replaced P&O by using ESC. Heydari-doostabad et al. [68] improved the tracking speed of ESC and the startup power drop, employing a method similar to that of [28] to rapidly move the OP close to the GMPP. This method exhibits satisfactory tracking speed; however, ESC calculation is complex, the internal high-pass filter is susceptible to noise interference, and actual implementation is difficult. In addition, ESC replaced P&O to provide the control signal required for the power switch, hindering ESC integration into traditional PGS firmware. Consequently, this method is limited to simulation in current literature, and actual experimental data cannot be provided.

3.1.4.2. *Model predictive control method.* The model predictive control (MPC) method can be used to forecast future events and implement controls based on those forecasts; therefore, MPC involves optimizing based on the control quantity required in the current situation. Bouilouta et al. [69] combined MPC and large-step GMPP search to address PSC problems. The MPC

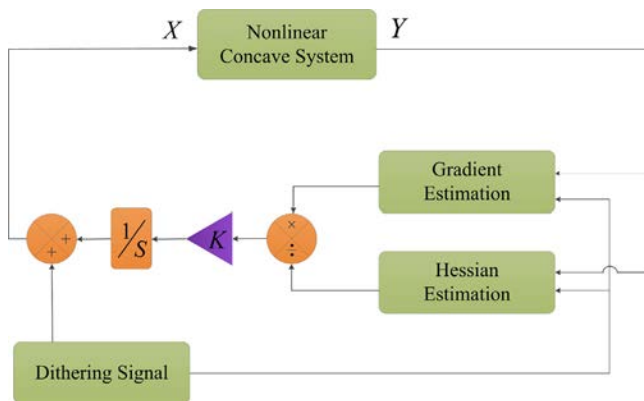


Fig. 19. The block diagram of ESC.

method exhibits favorable tracking speed and accuracy, although complex calculations are required. Furthermore, the MPC design parameters are related to the system model and the power converter topology. Compared with MPC, the design of other methods need not take the power converter topology into account; thus, actual implementation of MPC is system dependent and difficult. Consequently, work in [69] only provided simulated results.

3.1.5. Comparing firmware-based methods

In this subsection, a simple comparison will be conducted, incorporating the journal papers that used the aforementioned firmware-based methods suitable for use in centralized architecture. The comparison addresses the dependence on system architecture, tracking speed, probability of successfully finding the GMPP, complexity of implementation, and sensors required. Table 1 summarizes the comparison results, providing a reference for PGS-designers and researchers during method selection.

3.1.6. Methods for detecting partial shading condition

The method for detecting PSC is often overlooked in GMPPT-related literature mainly because the transient state of various operating conditions need not be considered (e.g., operating conditions changing from uniform insolation to PSC or vice versa) when writing a paper. However, PGS design engineers must be able to detect whether the current system is exposed to uniform insolation or PSC, and whether the system operating condition changed. Because MPPT techniques for handling PSC problems must address numerous factors, such techniques are typically slower compared with traditional, rapid MPPT methods (e.g., the variable-step P&O method). Therefore, an accurate understanding of the current operating status facilitates selecting suitable algorithms and avoiding extending the tracking time. In this subsection, the PSC detection methods proposed by the references listed in Table 1 are compared. Table 2 summarizes the comparison results, showing whether the proposed detection methods can accurately distinguish between uniform insolation and PSC, and whether they can determine if the GMPP changed and subsequently reinitialize tracking for the five possible operating condition changes. Fig. 20 shows the five possible changes in operating condition tested in this study.

Table 1  
Comparison of firmware-based methods.

Method	Dependence on system	Tracking speed	Hit count	Algorithm complexity	Sensors required	Notes
[26–28]	Y	Fast	Low	Low	V, I	
[30]	N	Slow	Medium	Medium	V, I	
[31]	N	Medium (relate to alpha)	Medium to high	Low	V, I	Can easily be integrated to original PGS
[32],[33]	N	Fast	Medium to high	Low	V, I	Can easily be integrated to original PGS
[36]	N	Fast	High	Medium	V, I	Requires recursive operation
[37],[38]	N	Fast	High	Medium	V, I	Requires recursive operation
[43], [44]	Y	Fast	Relate to the completeness of the training data	Low to medium	Irradiance Temperature	
[47]	N	Fast	Medium to high	Medium	V, I	
[49]	N	Slow to medium	High	Medium to high	V, I	Stochastic process
[53]	N	Slow to medium	High	Medium to high	V, I	Stochastic process
[57–60]	N	Slow to medium	High	Medium	V, I	Stochastic process
[67]	N	Slow to medium	High	Medium to high	V, I	Stochastic process

**Table 2**  
Comparing PSC detection methods.

Method	Ref.	Parameter description	Case I		Case II		Case III		Case IV		Case V	
			Reinitial	Uniform/Non-uniform	Reinitial	Uniform/Non-uniform	Reinitial	Uniform/Non-uniform	Reinitial	Uniform/Non-uniform	Reinitial	Uniform/Non-uniform
$\frac{I(S_{k+1})-I(S_k)}{I(S_k)} > \Delta I$	[53]	$I(S_{k+1})$ : The current of the $(k+1)$ -th iteration	Yes	No	Yes	No	Yes	No	Yes	No	No	No
$\frac{P(k+1)-P(k)}{P(k)} > \Delta P$	[59]	$I(S_k)$ : The current of the $k$ -th iteration $\Delta I$ : A pre-defined constant $P(k+1)$ : The power of the $(k+1)$ -th iteration	Yes	No	Yes	No	Yes	No	Yes	No	No	No
$V(k+1)-V(k) < \Delta V$ $\frac{P(k+1)-P(k)}{P(k)} > \Delta P$	[49]	$P(k)$ : The power of the $k$ -th iteration $\Delta P$ : A pre-defined constant $V(k+1), P(k+1)$ : The voltage/power of the $(k+1)$ -th iteration	Yes	No	Yes	No	Yes	No	Yes	No	No	No
$ V(k+1)  < -\Delta V$ $\frac{P(k+1)-P(k)}{P(k)} > \Delta P$	[56]	$V(k), P(k)$ : The voltage/power of the $k$ -th iteration $\Delta V, \Delta P$ : Pre-defined constants $V(k+1), P(k+1)$ : The voltage/power of the $(k+1)$ -th iteration	Yes	No	Yes	No	Yes	No	Yes	No	No	No
$\frac{I_{d1}-I_{d2}}{I_{d3}} \geq 0.1$ $\frac{V_{d1}-V_{d2}}{V_{d1}} \geq 0.2$	[36]	$P(k)$ : The power of the $k$ -th iteration $\Delta P$ : Pre-defined constants $V_{d1}, I_{d1}$ : The voltage/current sample of point 1 (in the middle)	Yes	Yes	Yes	Yes	Yes	Yes	Yes	Yes	No	No
$P'_k(x_{2-d}) = \frac{P_k(x_{2-d})-P_{k-1}(x_{1+d})}{2}$ $\frac{P_k(x_{2-d})-P_{k-1}(x_{1+d})}{P'_k(x_{2-d})} < r$	[57] [60] [31,37]	$V_{d2}, I_{d2}$ : The voltage/current sample of point 2 (at the left side) $V_{d3}, I_{d3}$ : The voltage/current sample of point 3 (at the right side) $d$ : The searching direction	Yes	Yes	Yes	Yes	Yes	Yes	Yes	Yes	No	No
$\Delta P > \Delta P_{crit}$	[30,33]	$P_k(x_{2-d})$ : New obtained power $P_{k-1}(x_{1+d})$ : Previous obtained power $P'_k(x_{2-d})$ : Averaged power $r$ : A pre-defined constant $\Delta P$ : The variation of the power	Yes	No	Yes	No	Yes	No	Yes	No	No	No

$\Delta P_{crit}$ : A pre-defined constant  
 $V(k), I(k)$ : The voltage/current of the k-th iteration

$$\Delta I_{SET} \approx \frac{I(k-1)}{N_p}$$

$$\Delta V = V(k) - V(k-1) < \Delta V_{SET}$$

$$\frac{\Delta I}{I(k-1)} = \left| \frac{I(k) - I(k-1)}{I(k-1)} \right| < \Delta I_{SET}$$

$V(k-1), I(k-1)$ : The voltage/current of the (k-1)-th iteration  
 $\Delta V, \Delta I, \Delta V_{SET}, \Delta I_{SET}$ : Pre-defined constants

$I_{MPP}$ : MPP current

$$\Delta I = I_{MPP} - I_c$$

$$\left( \frac{\Delta I}{I_c} \right)_u > \left( \frac{\Delta I}{I_c} \right)_{around V_{array} = 0.8N_s V_{oc}}$$

$I_c$ : Current at a point near MPP

$\Delta I$ : Pre-defined constants

No

No

Yes

Yes

Yes

Yes

Yes

Yes

Yes

Yes

Yes

Yes

Yes

Yes

Yes

Yes

Yes

Yes

Yes

Yes

No

No

Yes

Yes

Yes

Yes

Yes

Yes

Yes

Yes

Yes

Yes

Yes

Yes

Yes

Yes

Yes

Yes

Yes

Yes

### 3.2. Hardware-based GMPPT techniques

In addition to using firmware-based methods to address the multiple peak values caused by PSCs, many researchers have proposed using hardware methods to solve this problem. These methods are simply discussed as follows.

#### 3.2.1. Investigation on system configuration and reconfiguration technique

If unmanaged, PSC cause the useable power of a system to decrease. Works in [70–72] studied the three configuration methods used in large PGSs, including series-parallel (SP), bridge-linked (BL), and total-crossed-tied (TCT). The results showed that in PSC, TCT and BL attain superior performance compared with SP. Comparing TCT and BL, TCT produces more power. Furthermore, works in [73] and [74] proposed immediately adjusting the configuration of PV arrays according to the shading pattern to compensate for the power losses caused by PSC. Although reconfiguration method can mitigate the effects of PSC, this technique requires using a switch matrix to implement architecture changes; therefore, the system is expensive and the controller design is complex. In addition, reconfiguration technique cannot guarantee the successful tracking of GMPP in all shading patterns. Ref. [75] and Ref. [76] are conference papers discussed system configurations, whereas Ref. [77–81] are conference papers explored using the reconfiguration method to reduce the effects of PSC.

#### 3.2.2. Multi-level converter

When a system adopts centralized architecture as shown in Fig. 4(a), a multi-level converter can be used when each PV module in the PGS must be independently controlled [82–84]. Multi-level converter can address PSC problems; however, because its number of levels is proportional to the number of series-connected PV modules in a PGS, after the architecture of PGS changes, the entire hardware system and controller must be re-designed. In addition, the greater the number of series-connected modules is, the more power semiconductor devices are required, increasing costs and power losses. Ref. [85–89] are conference papers explored multi-level converters.

#### 3.2.3. Distributed architecture

Fig. 4(b)–(d) show that in addition to using a centralized architecture, a PGS can be designed to apply a DC/DC converter or DC/AC inverter for each PV module. This architecture is called a distributed architecture. Because each power circuit has its own designated controller, even if PV modules in the system experience various levels of shading, the distributed architecture can continue to track the GMPP of the entire system. Typically, when a DC/DC converter is attached to the back of the PV module as shown in Fig. 4(b) and (c), this architecture is called a module-integrated converter (MIC) [90–96]. Conversely, when a DC/AC inverter is attached to the back of the PV module as shown in Fig. 4(d), this architecture is often called a micro-inverter [97]. Distributed architecture can guarantee tracking of the system GMPP; furthermore, because its control is distributed, the reliability and robustness of the system increase. However, the hardware costs of distributed architecture are often high, and implementing the controller is complex and requires a high processing speed microcontroller. In addition, because micro-inverters are directly connected to the utility, the hardware design must address grid-interconnection and safety problems [97]. Ref. [98–104] are conference papers studied MICs, whereas Ref. [105–107] are conference papers explored micro-inverters.



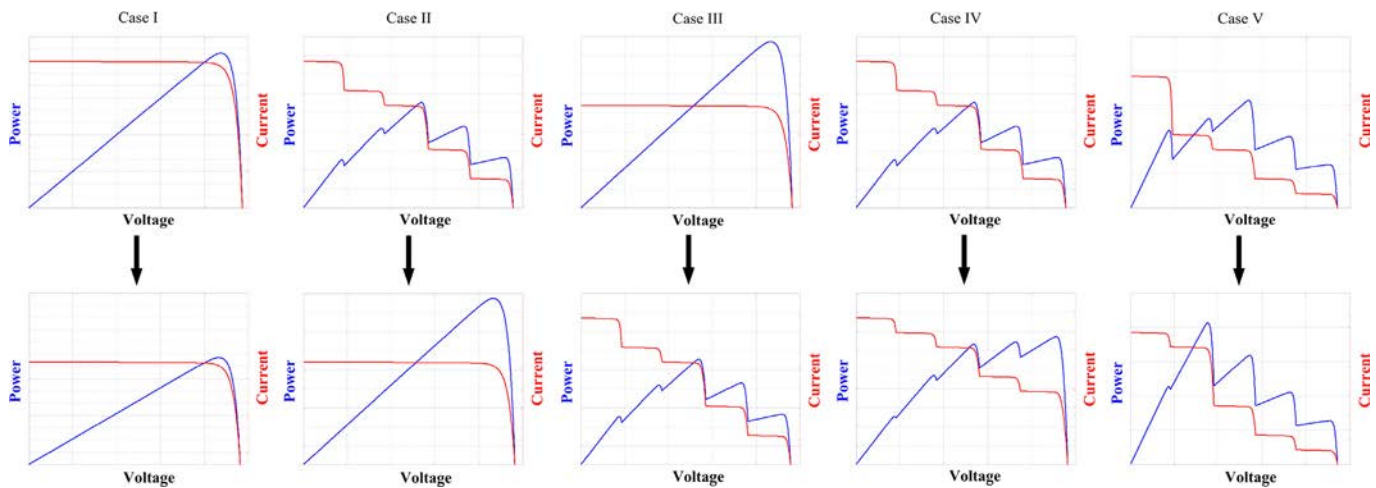


Fig. 20. The five possible changes in operating mode tested in this study.

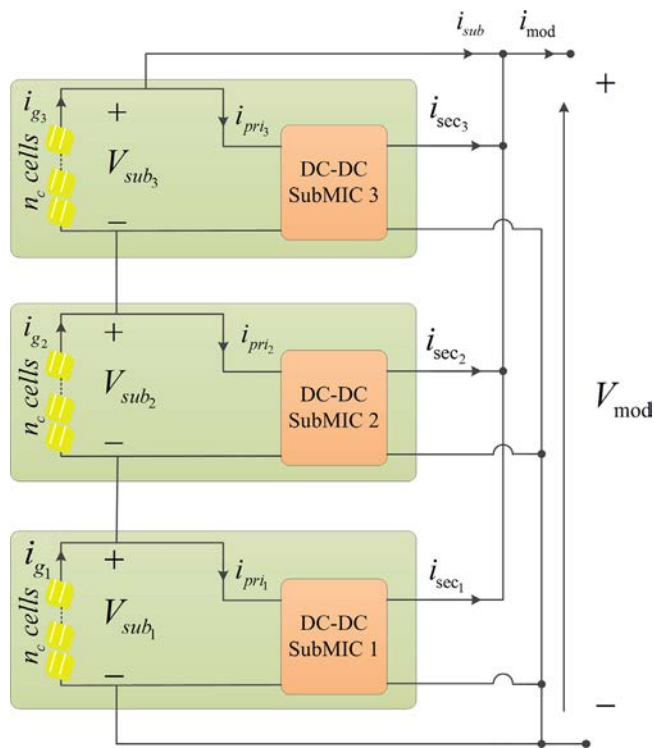


Fig. 21. Equalizer-assisted architecture.

### 3.2.4. Equalizer-assisted architecture

Equalizer-assisted architecture as shown in Fig. 21 has been a popular method of addressing PSC problems in the past two years. Fig. 21 shows that the operating principle of this method is similar to the parallel-connected MIC shown in Fig. 4(b). The primary difference is that parallel-connected MIC must process all the power supplied by the PV module, whereas the equalizer-assisted architecture must only process the power difference between unbalanced PV modules. Therefore, this architecture guarantees tracking of the system GMPP and its hardware costs are less compared with that of the parallel-connected MIC method [108–112]. Because this method is similar to the equalizer used in the series-connected batteries of electric vehicles, researchers have called this architecture a PGS equalizer. The advantages and disadvantages of this method are the same as those of distributed architecture. Conference paper [113] also examined equalizer-assisted architecture.

### 3.2.5. Summary and comparison of hardware methods

Previous descriptions show that numerous types of hardware architecture can solve or mitigate PSC problems. Because hardware-based solutions relate to the selection of power converters, which must be designed to address system specifications and power ratings, and most system specifications used in literature are distinct. Therefore, no further in-depth discussions are conducted regarding hardware-based solutions; however, relevant information regarding such solutions is summarized in Table 3.

## 4. Simulated results of selected methods

The number of references and the number of citations demonstrated that the most commonly used firmware-based techniques for addressing PSC were the two-stage, segmental search, and SC methods. In this subsection, five representative methods were selected and MATLAB was employed to test these methods and perform comparisons. The methods selected in this study were Ref. [28] (representing the system characteristic curve method, cited 73 times), Ref. [30] (the most cited method, cited 215 times), Ref. [32] (representing the two-stage searching method, cited 19 times), Ref. [36] (representing the segmental search method, cited 55 times), and Ref. [58] (representing the SC method, cited 45 times). Because the parameter settings of [30] and [32] influenced the GMPPT performance, simulations of [30] and [32] were conducted using different parameter settings to assess the tracking performance. Table 4 lists the various methods and relevant parameter setting values. In Section 2, it was demonstrated that distinct shading patterns produce distinct P–V characteristic curves. However, most references tested only a few specific shading patterns; thus, the proposed methods cannot be guaranteed suitable for all possible shading patterns. In this study, simulations were performed based on a 5s1p system constituting five Sun Power E19/240 PV modules, and MATLAB was used to simulate 100–1000 W/m<sup>2</sup> of irradiance levels on each module in 100 W/m<sup>2</sup> increments. Consequently, each module had 10 possible irradiance levels. To produce a P–V characteristic curve that exhibited five peak values in a 5s1p system, the irradiance level for each module must be distinct. In five series-connected modules that exhibit different irradiance levels, there are  $C(10,5)=252$  possible shading patterns. Therefore, the eight methods listed in Table 4 were tested using all 252 possible shading patterns in this paper. Table 5 lists the results. The specification of the PV module used in this study is summarized in Table 6.

**Table 3**  
Comparison of hardware-based methods.

Method	Advantage	Disadvantage
Investigation on system configuration [70–72] Reconfiguration methods [73–74]	No hardware required No power converter required	Can only mitigate PSC effect Cannot guarantee GMPP tracking High system cost Complicated control
Multi-level converter [82–84]	MPPT for individual PV module	Individual PV modules may not operate at their MPP. System should be re-designed when PGS architecture changes High switching loss
Distributed power structure (series/parallel MIC) [90–96]	MPPT for individual PV module High GMPPT accuracy System upgradable	Higher hardware costs Complicated control
Distributed power structure (micro-inverter) [97]	MPPT for individual PV module High GMPPT accuracy System upgradable Compact size	Higher hardware costs Complicated control Grid-interconnection issues should be taken into account
Balancer auxiliary structure [108–112]	MPPT for individual PV module High GMPPT accuracy Only process the power difference between mismatched PV modules System upgradable Compact size	Higher hardware costs Complicated control

**Table 4**  
The methods simulated in this study and their corresponding parameter settings.

Method	Ref.	Initial Settings
Method 1	36	P&O perturbation step in 2nd stage: 1.0 V
Method 2	30	Search step in 1st stage: $0.6 V_{oc,one}$ P&O perturbation step in 2nd stage: 1.0 V
Method 3	30	Search step in 1st stage: $0.7 V_{oc,one}$ P&O perturbation step in 2nd stage: 1.0 V
Method 4	30	Search step in 1st stage: $0.8 V_{oc,one}$ P&O perturbation step in 2nd stage: 1.0 V
Method 5	32	Search step in 1st stage: 20 W P&O perturbation step in 2nd stage: 1.0 V
Method 6	32	Search step in 1st stage: 50 W P&O perturbation step in 2nd stage: 1.0 V
Method 7	28	N.A.
Method 8	59	$\omega=0.4, c_1=1.2, c_2=1.6$

In Table 5, hit\_count refers to the number of successful times the GMPP was located during the 252 tests. Because the second stages of [28], [30], and [32] used P&O (locating MPP using P&O yields oscillations), tracking success was defined as the located MPP being 99.8% larger than the actual GMPP; otherwise, the result was regarded as tracking failure. In certain shading patterns, the difference between the highest and second highest peaks in the P–V characteristic curve was small (such as shading pattern [800 W/m<sup>2</sup>, 400 W/m<sup>2</sup>, 300 W/m<sup>2</sup>, 200 W/m<sup>2</sup>, 100 W/m<sup>2</sup>], GMPP=203.9 W, second highest peak=195.0 W); this can cause errors in certain GMPPT methods. However, the difference in the obtained power will be small if the system tracks the second highest peaks instead of the highest ones. Consequently, obtaining results that presented a low hit\_count and a relatively high output power was likely. Therefore, tracking accuracy should also be taken into account for performance evaluation. Table 5 lists a comparison of tracking accuracy for the eight methods. In Table 5, avg\_acc refers to the average accuracy value of MPP tracking for the 252 tests; that is,  $\sum_{n=1}^{252} MPP_{acc,n}/252$ , and  $MPP_{acc,n}$  is defined as the ratio of the MPP found by the algorithm divided by the actual GMPP in the  $n^{th}$  test. Similarly, max\_acc and min\_acc refer to the maximal and

minimal values of the 252 test results, respectively. In addition to tracking accuracy, tracking speed is also critical to system design. When comparing tracking speeds of existing methods, many researchers have compared actual tracking times (unit in seconds); however, unless the PGS specifications and power converter of two systems are identical (indicating that the hardware settling time is consistent), this comparison provides no value. For example, the practical design of an MPPT system must address the settling time of power circuits to select the interval between two sampling times. If the sampling speed is faster compared with the system settling time, the value of the voltage and current sampled by the algorithm does not indicate steady state, and thus cannot be used to assess the effects generated by the control command. However, the settling time of a low-power switching converter is shorter than that of a high-power one. Therefore, despite using identical GMPPT algorithms, the tracking time of a low-power system may be shorter compared with that of a high-power system. In other words, assessing the tracking speed of MPPT methods by comparing tracking times but without considering other factors produces biased results. Therefore, the authors of this paper propose that the number of iterations required (related to only the method) rather than the time (related to the system and the method) should be used to compare tracking speeds. Iteration refers to the number of times a specific function is calculated. Using the P&O method as an example, one iteration refers to one perturbation. In another example, the number of iterations is the number of MPP calculation interrupts when a proposed method is implemented by microcontrollers. In Table 5, avg\_step refers to the average number of required iterations for tracking the MPP in the 252 tests. Similarly, max\_step and min\_step refer to the maximal and minimal required iteration numbers in the 252 MPPT tests, respectively. Of the eight testing methods, only Method 8 (PSO algorithm) exhibited stochastic characteristics; that is, the tracking results obtained in each execution could vary. Thus, test results of Method 8 provided in Table 5 is the average of 20 repeated tests using the same shading pattern; consequently, the max\_step and min\_step of Method 8 are not integer numbers.

From Table 5, the following can be concluded:

- 1) P&O, IncCON, and variable-step P&O/IncCON are the most commonly used methods in the second stage of the two-stage method. Therefore, the performance of the two-stage

**Table 5**  
Simulated results.

	Direct	Patel_0.6	Patel_0.7	Patel_0.8	Power_20	Power_50	Real	PSO
avg_MPPT_acc (%)	98.99	51.36	51.35	98.41	99.85	99.45	52.09	99.96
max_MPPT_acc (%)	100.00	100.00	100.00	100.00	100.00	100.00	99.79	100.00
min_MPPT_acc (%)	92.48	17.43	17.43	68.51	96.69	81.21	31.45	99.20
hit_count	183	11	11	153	227	215	1	251.85
avg_MPPT_step	20.94	71.44	71.87	473.15	33.98	23.58	42.26	129.19
max_MPPT_step	31.00	102.00	112.00	1185.00	53.00	38.00	47.00	700.00
min_MPPT_step	16.00	60.00	65.00	38.00	19.00	13.00	22.00	7.00

**Table 6**  
The specification of the sun power E19/240 PV module.

Parameters for model	
Maximum power ( $P_{max}$ )	240 W
Open circuit voltage ( $V_{oc}$ )	48.6 V
MPP voltage ( $V_{mp}$ )	40.5 V
Short circuit current ( $I_{sc}$ )	6.30 A
MPP current ( $I_{mp}$ )	5.93 A
Temperature coefficient ( $\alpha_v$ )	-132.5 mV/K

method is determined mainly based on the first-stage (GMPP location search).

- The probability of finding the GMPP by using a system characteristic curve method, which is based on PV panel equivalent resistance, is relatively low. In [28], when PSC yielded a complex  $P$ - $V$  characteristic curve (increasing the number of LMPPs), the probability of this method finding the GMPP significantly decreased (1/252). Thus, this method should only be used for simple  $P$ - $V$  characteristic curves (when used to assess a 2s1p system, this method can yield a 20/45 probability of success with avg\_acc=85.42%).
- The method used in [30] attained the highest number of citations in current GMPPT paper. However, this method is designed after observing the  $P$ - $V$  characteristic curve caused by PSC and converting such observations into simplified search rules. Thus, the probability of finding the GMPP is also low. The performance and design considerations of this method are outlined as follows: (1) in [30], the author recommended using a 0.6–0.7  $V_{oc,one}$  step to conduct jump search. However, extensively testing by using a 5s1p system assembled from Sun Power E19/240 PV modules showed that 0.8  $V_{oc,one}$  yielded better results. Therefore, prior to using this method, simple analysis on system characteristics or parameter setting experiments should be conducted to determine the optimal design parameters; (2) Although the hit\_count (153/252) for this method was not high, the avg\_acc result (98.41%) indicated a high level of tracking accuracy, suggesting that this method did not track the real GMPP, but the power of the tracked LMPP was not substantially different compared with the power of the GMPP. In other words, from the perspective of electricity sales profit, this method is worth adopting; and (3) Table 5 shows that large numbers of steps are required in this method (473.15), indicating that the tracking time is relatively long. Because this method uses P&O to track each LMPP, improving this procedure can enhance tracking speed.
- The method in [32] is another representative method of the two-stage searching method. The simulated results showed that this method attained excellent hit counts, tracking accuracy, and tracking time. The primary difference between this method and that used in [30] was that this method involves only a brief scan of the  $P$ - $V$  characteristic curve in the first stage; therefore, the slow tracking speed encountered in [30] (using P&O to track each LMPP reduces tracking speed) can be

avoided. The simulated results of this method indicated that when large steps were selected for the sweep ( $\Delta P=50$  W), the system required decreased time to find the GMPP (23.58 steps), but could miss the GMPP (hit\_count=215). Conversely, when small steps were selected ( $\Delta P=20$  W), the system had a high probability of finding the GMPP (hit\_count=227), but required a relatively long time (33.98 steps). Therefore, using this method requires addressing the tradeoff between step size and search time. Because this method is simple to implement and can be readily integrated into original PGS firmware, it is a method worth using, implying two directions of future study. First, finding a sweeping rule that can improve hit\_count, and second, improving the P&O method used in the second stage to enhance the GMPPT speed (such as using variable-step P&O).

- The method in [36] can also be used to balance hit count, tracking accuracy, and tracking time; however, this method cannot be easily integrated with original PGS firmware (typically requiring complete algorithm re-write), making it only suitable for use in newly developed PGSS. Although the mathematical principle of this method is relatively simple and comprehensive, actual coding yields challenges. First, the jump range for sampling points used in this method ( $V_{A1} \rightarrow V_{A2} \rightarrow V_{A3}$ , see Fig. 13) is the largest of the five methods tested, indicating that the firmware designer must consider the hardware settling time to avoid excessive stress on the power switch. In addition, this method involves using the recursive method to gradually reduce the search range; this challenges some firmware engineers who are only accustomed to sequential programming.
- The method in [58] represents the SC method. According to the simulated results, the tracking accuracy of this method was 100% (hit\_count=252). Because PSO can be applied to problems more complex than those examined in this study (e.g., the traveling salesman problem), this result was unsurprising. Additionally, the avg\_acc of this method was the highest of the tested methods, indicating that this method yielded the highest electricity sales profit. However, based on the simulated results, this method required a relatively long tracking time; therefore is unsuitable for use in areas that exhibit rapid shading pattern changes. Because PSO is a stochastic optimization method, the number of iterations required to track the GMPP for each execution may be different; this distinguishes SC from the other methods. Furthermore, the parameters in (16) and (17) substantially affect the tracking performance when this method is used. Consequently, optimizing these parameters is a topic worth studying. According to [59] and [60], SC can be implemented by employing low-cost microcontrollers such as TMS320 or dsPIC33 series digital signal controllers.

## 5. Conclusion

Extensive recent literature shows that the GMPPT methods suitable for use in PSC remain a popular research topic. Current



literature comprises numerous algorithms and hardware architectures related to addressing PSC problems; therefore, PGS designers may be challenged to select appropriate firmware or hardware architecture. In this study novel GMPPT techniques from diverse references were collected, classified, compared, and summarized; the advantages and disadvantages of these techniques are displayed in tables. Regarding firmware-based techniques, comparisons were conducted and the indices that must be considered in the design were summarized such as dependence on system architecture, tracking speed, the probability of successfully tracking the GMPP, algorithm complexity, and required sensors. The advantages and disadvantages of the hardware-based techniques were also discussed. Furthermore, PSC detection and determination methods, which have seldom been discussed in current literature, were reviewed and compared. Finally, MATLAB was used to extensively simulate five commonly used GMPPT algorithms and explore their tracking performance; recommendations were then proposed for using these methods. Based on the simulated results, topics worth studying were also suggested. Firmware-based GMPPT methods can continue to be enhanced, particularly in terms of maintaining hit count and tracking accuracy while accounting for tracking speed, as well as addressing problems related to uniform insolation and PSC and detecting the transient state in an actual system. To conclude, this study should serve as a valuable reference for PGS researchers and application engineers.

## Acknowledgments

The research underlying this paper was supported by The Construction and Promotion Plan for Million Rooftop PVs Project (103-DO304). The authors are grateful for the Bureau of Energy.

## References

- Gaëtan M, Marie L, Manoël R, Theologitis IT, Myrto P. Global Market Outlook For Photovoltaics 2013–2017. In: Proceedings of the European Photovoltaic Industry Association, Belgium; 2013. p. 1–60.
- Esram T, Chapman PL. Comparison of photovoltaic array maximum power point tracking techniques. *IEEE Trans Energy Convers* 2007;22:439–49.
- Reisi AR, Moradi HM, Jamasb S. Classification and comparison of maximum power point tracking techniques for photovoltaic system: a review. *Renew Sustain Energy Rev* 2013;19:433–43.
- Subudhi B, Pradhan R. A comparative study on maximum power point tracking techniques for photovoltaic power systems. *IEEE Trans Sustain Energy* 2013;4:89–98.
- de Brito MAG, Galotto Jr. L, Sampaio LP, de Azevedo e Melo G, Canesin CA. Evaluation of the main MPPT techniques for photovoltaic applications. *IEEE Trans Ind Electron* 2013;60:1156–67.
- Bhatnagar P, Nema RK. Maximum power point tracking control techniques: state-of-the-art in photovoltaic applications. *Renew Sustain Energy Rev* 2013;23:224–41.
- Eltawil MA, Zhao Z. MPPT techniques for photovoltaic applications. *Renew Sustain Energy Rev* 2013;25:793–813.
- Ishaque K, Salam Z. A review of maximum power point tracking techniques of PV system for uniform insolation and partial shading condition. *Renew Sustain Energy Rev* 2013;19:475–88.
- Salam Z, Jubaer Ahmed, Merugu BS. The application of soft computing methods for MPPT of PV system: A technological and status review. *Appl Energy* 2013;107:135–48.
- Bidram A, Davoudi A, Balog RS. Control and Circuit Techniques to Mitigate Partial Shading Effects in Photovoltaic Arrays. *IEEE J Photovolt* 2012;2:532–46.
- Wang YJ, Hsu PC. Analytical modelling of partial shading and different orientation of photovoltaic modules. *IET Renew Power Gener* 2010;4:272–82.
- Paraskevadaki EV, Papanathanassion SA. Evaluation of MPP Voltage and Power of mc-Si PV Modules in Partial Shading Conditions. *IEEE Trans Energy Conversion* 2011;26:923–32.
- Patel H, Agarwal V. MATLAB-Based Modeling to Study the Effects of Partial Shading on PV Array Characteristics. *IEEE Transactions on Energy Conversion* 2011;23:302–10.
- Ishaque K, Salam Z, Taheri H, Syafaruddin. Modeling and simulation of photovoltaic (PV) system during partial shading based on a two-diode model. *Simulation Modelling Practice and Theory* 2011;19:1613–26.
- Ishaque K, Salam Z, Syafaruddin. A comprehensive MATLAB Simulink PV system simulator with partial shading capability based on two-diode model. *Solar Energy* 2011;85:2217–27.
- Kadri R, Andrei H, Gaubert JP, Ivanovici T, Champenois G, Andrei P. Modeling of the photovoltaic cell circuit parameters for optimum connection model and real-time emulator with partial shadow conditions. *Energy* 2012;42:57–67.
- Sánchez Reinoso CR, Milone DH, Buitrago RH. Simulation of photovoltaic centrals with dynamic shading. *Applied Energy* 2013;103:278–89.
- Bastidas JD, Franco E, Petrone G, Ramos-Paja CA, Spagnuolo G. A model of photovoltaic fields in mismatching conditions featuring an improved calculation speed. *Electric Power Syst Res* 2013;96:81–90.
- Orozco-Gutiérrez ML, Ramírez-Scarpetta JM, Spagnuolo G, Ramos-Paja CA. A technique for mismatched PV array simulation. *Renew Energy* 2013;55:417–27.
- Dolara A, Lazaroiu GC, Leva S, Manzolini G. Experimental investigation of partial shading scenarios on PV (photovoltaic) modules. *Energy* 2013;55:466–75.
- Martínez-Moreno F, Mun-oz J, Lorenzo E. Experimental model to estimate shading losses on PV arrays. *Sol Energy Mater Sol Cells* 2010;94:2298–303.
- Brecl K, Topic M. Self-shading losses of fixed free-standing PV arrays. *Renew Energy* 2011;36:3211–6.
- Poshtkouhi S, Palaniappan V, Fard M, Trescases O. A general approach for quantifying the benefit of distributed power electronics for fine grained MPPT in photovoltaic applications using 3-D modeling. *IEEE Trans Power Electron* 2012;27:4656–66.
- Sullivan CR, Averbuch JJ, Latham AM. Decrease in photovoltaic power output from ripple: simple general calculation and the effect of partial shading. *IEEE Trans Power Electron* 2013;28:740–7.
- Rodrigo P, Fernández Eduardo F, Almonacid F, Pérez-Higueras PJ. A simple accurate model for the calculation of shading power losses in photovoltaic generators. *Sol Energy* 2013;93:322–33.
- Kobayashi K, Takano I, Sawada Y. A study of a two stage maximum power point tracking control of a photovoltaic system under partially shaded insolation conditions. *Sol Energy Mater Sol Cells* 2006;90:2975–88.
- Carannante G, Fraddanno C, Pagano M, Piegari L. Experimental performance of MPPT algorithm for photovoltaic sources subject to inhomogeneous insolation. *IEEE Trans Ind Electron* 2009;56:4374–80.
- Ji YH, Jung DY, Kim JG, Kim JH, Lee TW, Won CY. A real maximum power point tracking method for mismatching compensation in PV array under partially shaded conditions. *IEEE Trans Power Electron* 2011;26:1001–9.
- Bifaretti S, Iacovone V, Cinà L, Buffone E. Global MPPT method for partially shaded photovoltaic modules. In: *Energy Conversion Congress and Exposition (ECCE)*; 2012. p. 4768–75.
- Patel H, Agarwal V. Maximum power point tracking scheme for PV systems operating under partially shaded conditions. *IEEE Trans Ind Electron* 2008;55:1689–98.
- Renaudineau H, Houari A, Martin JP, Pierfederici S, Meibody-Tabar F, Gerardin B. A new approach in tracking maximum power under partially shaded conditions with consideration of converter losses. *Sol Energy* 2011;85:2580–8.
- Koutroulis E, Blaabjerg F. A new technique for tracking the global maximum power point of PV arrays operating under partial-shading conditions. *IEEE J Photovolt* 2012;2:184–90.
- Kouchaki A, Iman-Eini H, Asaei B. A new maximum power point tracking strategy for PV arrays under uniform and non-uniform insolation conditions. *Sol Energy* 2013;91:221–32.
- Kashif MF, Choi S, Park Y, Sul SK. Maximum power point tracking for single stage grid-connected PV system under partial shading conditions. In: *Power Electronics and Motion Control Conference (IPEMC)*; 2012. p. 1377–83.
- Kouchaki A, Iman-Eini H, Asaei B. Maximum power point tracking algorithm based on *I-V* characteristic of PV array under uniform and non-uniform conditions. In: *Proceedings of the 2012 IEEE International Conference on Power and Energy (PECon)*; 2012. p. 331–36.
- Nguyen TL, Low KS. A global maximum power point tracking scheme employing DIRECT search algorithm for photovoltaic systems. *IEEE Trans Ind Electron* 2010;57:3456–67.
- Ahmeda NA, Miyatake M. A novel maximum power point tracking for photovoltaic applications under partially shaded insolation conditions. *Electric Power Syst Res* 2008;78:777–84.
- Ramaprabha R, Balaji M, Mathur BL. Maximum power point tracking of partially shaded solar PV system using modified Fibonacci search method with fuzzy controller. *Electr Power Energy Syst* 2012;43:754–65.
- Fan Y, Fang C, Liang Z. New GMPPT algorithm for PV arrays under partial shading conditions. In: *Proceedings of the 2012 IEEE international symposium on industrial electronics (ISIE)*; 2012. p. 1046–51.
- Escobar G, Ho CNM, Pettersson S. Maximum power point searching method for partial shaded PV strings. In: *Proceedings of the IECON 2012–38th Annual Conference on IEEE Industrial Electronics Society*; 2012. p. 5726–31.
- Liu YH, Liu CL, Huang JW, Chen JH. Neural-network-based maximum power point tracking methods for photovoltaic systems operating under fast changing environments. *Sol Energy* 2013;89:42–53.
- Akkaya R, Kulaksız AA, Aydoğdu O. DSP implementation of a PV system with GA-MLP-NN based MPPT controller supplying BLDC motor drive. *Energy Convers Manag* 2007;48:210–8.
- Syafaruddin Karatepe E, Hiyama T. Artificial neural network-polar coordinated fuzzy controller based maximum power point tracking control under partially shaded conditions. *IET Renew Power Gener* 2009;3:239–53.



- [44] Syafaruddin Karatepe E, Hiyama T. Performance enhancement of photovoltaic array through string and central based MPPT system under non-uniform irradiance conditions. *Energy Convers Manag* 2012;62:131–40.
- [45] Syafaruddin, Hiyama T, Karatepe E. Investigation of ANN performance for tracking the optimum points of PV module under partially shaded conditions. In: *IPEC 2010 Conference Proceedings*; 2010. p. 1186–91.
- [46] Karatepe E, Hiyama T, Boztepe M, Colak M. Voltage based power compensation system for photovoltaic generation system under partially shaded insolation conditions. *Energy Convers Manag* 2008;49:2307–16.
- [47] Alajmi BN, Ahmed KH, Finney SJ, Williams BW. A maximum power point tracking technique for partially shaded photovoltaic systems in microgrids. *IEEE Trans Ind Electron* 2013;60:1596–606.
- [48] Sayal A. MPPT techniques for photovoltaic system under uniform insolation and partial shading conditions. In: *Proceedings of the 2012 Students Conference on Engineering and Systems (SCES)*; 2012. p. 1–6.
- [49] Shaiek Y, Smida MB, Sakly A, Mimouni MF. Comparison between conventional methods and GA approach for maximum power point tracking of shaded solar PV generators. *Sol Energy* 2013;90:107–22.
- [50] Mohajeri HR, Moghaddam MP, Shahparasti M, Mohamadian M. Development a New Algorithm for Maximum Power Point Tracking of Partially Shaded Photovoltaic Arrays. In: *Proceedings of the 2012 20th Iranian Conference on Electrical Engineering (ICEE)*; 2012. p. 489–94.
- [51] Taheri H, Salam Z, Ishaque K, Syafaruddin. A. Novel maximum power point tracking control of photovoltaic system under partial and rapidly fluctuating shadow conditions using differential evolution. In: *2010 IEEE Symposium on Industrial Electronics & Applications (ISIEA)*; 2010. p. 82–87.
- [52] Tajuddin MFN, Ayob SM, Salam Z. Tracking of maximum power point in partial shading condition using differential evolution (DE). In: *Proceedings of the 2012 IEEE International Conference on Power and Energy (PECon)*; 2012. p. 384–89.
- [53] Jianga LL, Maskell DL, Patra JC. A novel ant colony optimization-based maximum power point tracking for photovoltaic systems under partially shaded conditions. *Energy Build* 2013;58:227–36.
- [54] Chowdhury SR, Saha H. Maximum power point tracking of partially shaded solar photovoltaic arrays. *Sol Energy Mater Sol Cells* 2010;94:1441–7.
- [55] Chen LR, Tsai CH, Lin YL, Lai YS. A biological swarm chasing algorithm for tracking the PV maximum power point. *IEEE Trans Energy Convers* 2010;25:484–93.
- [56] Miyatake M, Veerachary M, Toriumi F, Fujii N, Ko H. Maximum power point tracking of multiple photovoltaic arrays: a PSO approach. *IEEE Trans Aerosp Electron Syst* 2011;47:367–80.
- [57] Ishaque K, Salam Z, Shamsudin A, Amjad M. A direct control based maximum power point tracking method for photovoltaic system under partial shading conditions using particle swarm optimization algorithm. *Appl Energy* 2012;99:414–22.
- [58] Ishaque K, Salam Z, Amjad M, Mekhilef S. An improved particle swarm optimization (PSO)-based MPPT for PV with reduced steady-state oscillation. *IEEE Trans Power Electron* 2012;27:3627–38.
- [59] Liu YH, Huang SC, Huang JW, Liang WC. A particle swarm optimization-based maximum power point tracking algorithm for PV systems operating under partially shaded conditions. *IEEE Trans Energy Convers* 2012;27:1027–35.
- [60] Ishaque K, Salam Z. A deterministic particle swarm optimization maximum power point tracker for photovoltaic system under partial shading condition. *IEEE Trans Ind Electron* 2013;60:3195–206.
- [61] Kamejima T, Phimmason V, Kondo Y, Miyatake M. The optimization of control parameters of PSO based MPPT for photovoltaics. In: *Proceedings of the 2011 IEEE ninth international conference on power electronics and drive systems (PEDS)*; 2011. p. 881–3.
- [62] Phimmason V, Kondo Y, Kamejima T, Miyatake M. Verification of efficacy of the improved PSO-based MPPT controlling multiple photovoltaic arrays. In: *Proceedings of the 2011 IEEE ninth international conference on power electronics and drive systems (PEDS)*; 2011. p. 1015–19.
- [63] Keyrouz F, Georges S. Efficient multidimensional maximum power point tracking using bayesian fusion. In: *Proceedings of the 2011 2nd international conference on electric power and energy conversion systems (EPECS)*; 2011. p. 1–5.
- [64] Keyrouz F, Hamad M, Georges S. Bayesian fusion for maximum power output in hybrid wind-solar systems. In: *Proceedings of the 2012 3rd IEEE international symposium on power electronics for distributed generation systems (PEDG)*; 2012. p. 393–97.
- [65] Zhou L, Chen Y, Guo K, Jia F. New approach for MPPT control of photovoltaic system with mutative-scale dual-carrier chaotic search. *IEEE Trans Power Electron* 2011;26:1038–48.
- [66] Zheng Y, Wei C, Lin S. A maximum power point tracking method based on tabu search for pv systems under partially shaded conditions. In: *IET conference on renewable power generation (RPG 2011)*; 2011. p. 1–4.
- [67] Lei P, Li Y, Seem JE. Sequential ESC-based global MPPT control for photovoltaic array with variable shading. *IEEE Trans Sustain Energy* 2011;2:348–58.
- [68] Heydari-doostabad H, Keypour R, Khalghani MR, Khooban MH. A new approach in MPPT for photovoltaic array based on extremum seeking control under uniform and non-uniform irradiances. *Sol Energy* 2013;94:28–36.
- [69] Bouilouta A, Mellit A, Kalogirou SA. New MPPT method for stand-alone photovoltaic systems operating under partially shaded conditions. *Energy* 2013;55:1172–85.
- [70] Kaushika ND, Gautam NK. Energy Yield Simulations of Interconnected Solar PV Arrays. *IEEE Trans Energy Convers* 2003;18:127–34.
- [71] Karatepe E, Boztepe M, Colak M. Development of a suitable model for characterizing photovoltaic arrays with shaded solar cells. *Sol Energy* 2007;81:977–92.
- [72] Ghoddami H, Yazdani A. A single-stage three-phase photovoltaic system with enhanced maximum power point tracking capability and increased power rating. *IEEE Trans Power Deliv* 2011;26:1017–29.
- [73] Nguyen D, Lehman B. An adaptive solar photovoltaic array using model-based reconfiguration algorithm. *IEEE Trans Ind Electron* 2008;55:2644–54.
- [74] Velasco-Quesada G, Guinjoan-Gispert F. Electrical PV array reconfiguration strategy for energy extraction improvement in grid-connected PV systems. *IEEE Trans Ind Electron* 2009;56:4319–31.
- [75] de Oliveira Reiter RD, Michels L, Pinheiro JR, Reiter RA, Oliveira SVG, Péres A. Comparative analysis of series and parallel photovoltaic arrays under partial shading conditions. In: *Proceedings of the 2012 10th IEEE/IAS international conference on industry applications (INDUSCON)*; 2012. p. 1–.
- [76] El-Dein MZS, Kazerani M, Salama MMA. Optimal total cross tied interconnection for photovoltaic arrays to reduce partial shading losses. In: *Proceedings of the 2012 IEEE Power and Energy Society General Meeting*; 2012. p. 1–6.
- [77] Liu Y, Pang Z, Cheng Z. Research on an adaptive solar photovoltaic array using shading degree model-based reconfiguration algorithm. In: *Proceedings of the 2010 Chinese control and decision conference (CCDC)*; 2010. p. 2356–60.
- [78] Cheng Z, Pang Z, Liu Y, Xue P. An adaptive solar photovoltaic array reconfiguration method based on fuzzy control. In: *Proceedings of the 2010 8th World congress on intelligent control and automation (WCICA)*; 2010. p. 176–81.
- [79] Lin X, Wang Y, Yue S, Shin D, Chang N, Pedram M. Near-optimal dynamic module reconfiguration in a photovoltaic system to combat partial shading effects. In: *Proceedings of the 49th design automation conference DAC 2012*; 2012. p. 516–21.
- [80] Wang Y, Lin X, Kim Y, Chang N, Pedram M. Enhancing efficiency and robustness of a photovoltaic power system under partial shading. In: *Proceedings of the 13th international symposium on quality electronic design (ISQED'12)*; 2012. p. 592–600.
- [81] Vemuru S, Singh P, Niamat M. Analysis of photo voltaic array with reconfigurable modules under partial shading. In: *Proceedings of the 2012 38th IEEE photovoltaic specialists conference (PVSC)*; 2012. p. 001437–41.
- [82] Busquets-Monge S, Rocabert J, Rodríguez P. Multilevel diode-clamped converter for photovoltaic generators with independent voltage control of each solar array. *IEEE Trans Ind Electron* 2008;55:2713–23.
- [83] Abdalla I, Corda J, Zhang L. Multilevel DC-link inverter and control algorithm to overcome the PV partial shading. *IEEE Trans Power Electron* 2013;28:14–8.
- [84] Park Y, Sul SK, Lim CH, Kim WC, Lee SH. Asymmetric control of DC-link voltages for separate MPPTs in three-level inverters. *IEEE Trans Power Electron* 2013;28:2760–9.
- [85] Stala R. Individual MPPT of photovoltaic arrays with use of single-phase three-level diode-clamped inverter. In: *Proceedings of the 2010 IEEE international symposium on industrial electronics (ISIE)*; 2010. p. 3456–62.
- [86] de Oliveira Reiter RD, Michels L, Péres A, Oliveira SVG. Analysis of PV arrays for residential applications using a three-phase step-up isolated DC-DC converter with high-frequency transformer. In: *Proceedings of the IECON 2011–37th annual conference on IEEE industrial electronics society*; 2011. p. 1208–1213.
- [87] Essakiappan S, Krishnamoorthy HS, Enjeti P, Balog RS, Ahmed S. Independent control of series connected utility scale multilevel photovoltaic inverters. In: *Proceedings of the 2012 IEEE energy conversion congress and exposition (ECCE)*; 2012. p. 1760–6.
- [88] Zeng G, Cao M, Chen Y. A multi-functional utility interface of bipv systems based on cascade multilevel converter. *Energy Procedia* 2012;17:356–65.
- [89] Anand S, Fernandes BG. Multilevel open-ended transformer based grid feeding inverter for solar photovoltaic application. In: *Proceedings of the IECON 2012–38th annual conference on IEEE industrial electronics society*; 2012. p. 5738–43.
- [90] Walker GR, Sernia PC. Cascaded DC-DC converter connection of photovoltaic modules. *IEEE Trans Power Electron* 2004;19:1130–9.
- [91] Román E, Alonso R, Ibañez P, Elorduizaparietxe S, Goitia D. Intelligent PV module for grid-connected PV systems. *IEEE Trans Ind Electron* 2006;53:1066–73.
- [92] Femia N, Lisi G, Petrone G, Spagnuolo G, Vitelli M. Distributed maximum power point tracking of photovoltaic arrays: novel approach and system analysis. *IEEE Trans Ind Electron* 2008;55:2610–21.
- [93] Roman E, Martinez V, Jimeno JC, Alonso R, Ibañez P, Elorduizaparietxe S. Experimental results of controlled PV module for building integrated PV systems. *Sol Energy* 2008;82:471–80.
- [94] Gao L, Dougal RA, Liu S, Iotova AP. Parallel-connected solar pv system to address partial and rapidly fluctuating shadow conditions. *IEEE Trans Ind Electron* 2009;56:1548–56.
- [95] Bratcu AI, Munteanu I, Bacha S, Picault D, Raison B. Cascaded DC-DC converter photovoltaic systems: power optimization issues. *IEEE Trans Ind Electron* 2011;58:403–11.
- [96] Pilawa-Podgurski RCN, Perreault DJ. Submodule integrated distributed maximum power point tracking for solar photovoltaic applications. *IEEE Trans Power Electron* 2013;28:2957–67.
- [97] Rodríguez CT, de la Fuente DV, Garcerá G, Figueres E, Moreno JAG. Reconfigurable control scheme for a PV microinverter working in both grid-connected and island modes. *IEEE Trans Ind Electron* 2013;60:1582–95.

- [98] Bellini A, Bifaretti S, Iacovone V. MPPT algorithm for current balancing of partially shaded photovoltaic modules. In: Proceedings of the 2010 IEEE international symposium on industrial electronics (ISIE); 2010. p. 933–8.
- [99] Abdel-Rahim O, Orabi M, Ahmed ME. Development an efficient photovoltaic (PV) configuration for low power applications. In: Proceedings of the 2010 IEEE international conference on power and energy (PECon); 2010. p. 622–7.
- [100] Zhang Q, Sun X, Zhong Y, Matsui M. A novel topology for solving the partial shading problem in photovoltaic power generation system, In: Proceedings of the IEEE 6th international power electronics and motion control conference, 2009 (IPEMC'09); 2009. p. 2130–5.
- [101] Poshtkouhi S, Trescases O. Multi-input single-inductor DC-DC Converter for MPPT in Parallel-Connected Photovoltaic Applications. In: Proceedings of the 2011 twenty-sixth annual IEEE applied power electronics conference and exposition (APEC); 2011. p. 41–7.
- [102] Peter PK, Agarwal V. A compact switched capacitor dc-dc converter based Global Peak Power Point tracker for partially shaded PV arrays of portable equipment, In: 2011 37th IEEE Photovoltaic Specialists Conference (PVSC), 2011, p. 000194–9.
- [103] Takahashi K, Matsumoto S. A novel small-capacity photovoltaic module for mobile applications. In: Proceedings of the 2011 37th IEEE photovoltaic specialists conference (PVSC); 2011. p. 003221–4.
- [104] Dhopley SV, Belly R, Ehlmannz J, Davoudix A, Chapmanz PL, Domínguez-García AD. A global maximum power point tracking method for PV module integrated converters, In: Proceedings of the 2012 IEEE energy conversion congress and exposition (ECCE); 2012. p. 4762–7.
- [105] Hester RK, Thornton C, Dhople S, Zhao Z, Sridhar N, Freeman D. High efficiency wide load range buck/boost/bridge photovoltaic microconverter, In: 2011 twenty-sixth annual IEEE applied power electronics conference and exposition (APEC); 2011. p. 309–13.
- [106] Johnson B, Krein P, Chapman P. Photovoltaic AC module composed of a very large number of interleaved inverters. In: Proceedings of the 2011 twenty-sixth annual IEEE applied power electronics conference and exposition (APEC); 2011. p. 976–81.
- [107] Imtiaz AM, Khan FH. AC solar cells: an embedded “All in one” PV power system, In: Proceedings of the 2012 twenty-seventh annual IEEE applied power electronics conference and exposition (APEC); 2012. p. 2053–9.
- [108] Villa LFL, Ho TP, Crebier JC, Raison B. Power electronics equalizer application for partially shaded photovoltaic modules. *IEEE Trans Ind Electron* 2013;60:1179–90.
- [109] Stauth JT, Seeman MD, Kesarwani K. Resonant switched-capacitor converters for sub-module distributed photovoltaic power management. *IEEE Trans Power Electron* 2013;28:1189–98.
- [110] Chong BVP, Zhang L. Controller design for integrated PV-converter modules under partial shading conditions. *Sol Energy* 2013;92:123–38.
- [111] Shenoy PS, Kim KA, Johnson BB, Krein PT. Differential power processing for increased energy production and reliability of photovoltaic systems. *IEEE Trans Power Electron* 2013;28:2968–79.
- [112] Olalla C, Clement D, Rodriguez M, Maksimovic D. Architectures and control of submodule integrated DC-DC converters for photovoltaic applications. *IEEE Trans Power Electron* 2013;28:2980–97.
- [113] Salam Z, Ramli MZ. A simple circuit to improve the power yield of PV array during partial shading. In: Proceedings of the 2012 IEEE energy conversion congress and exposition (ECCE); 2012. p. 1622–6.